Available online at www.sciencedirect.com

ScienceDirect

Procedia CIRP 48 (2016) 489 – 494

www.elsevier.com/locate/procedia

23rd CIRP Conference on Life Cycle Engineering

Development of software tool for cellular structure integration for additive manufacturing

Supachai Vongbunyong[a]*, Sami Kara[b]

[a]*Institute of Field Robotics, King Mongkut's University of Technology Thonburi, Thailand*
[b]*School of Mechanical and Manufacturing Engineering, The University of New South Wales, Australia*

* Corresponding author. Tel.: +66 (0) -2470-9339; fax: +66 (0) -2470-9703. *E-mail address:* supachai_von@fibo.kmutt.ac.th

Abstract

Cellular structure is one of the solutions for producing parts in a more resource efficient way by reduction of material and time used. Recent advances in Additive Manufacturing (AM) have enabled these complex structures to be built while it is almost impossible by subtractive manufacturing. However, modelling process is resource intensive and time consuming due the geometrical complexity. This article presents development of a software tool for rapidly modelling the structures with prefabrication hybrid geometric modelling (P-HGM) method based on a hybrid B-Rep approach. The structure will be integrated to the specified volume in the base 3D model with polygonal approach. Open-source libraries, including OpenCascade Technology (OCCT) and Visualization Toolkits (VTK), are used.

Keywords: Cellular Structure; Additive Manufacturing; Sustainable Manufacturing; Rapid Prototyping; CAD; Hybrid B-Rep; Geometry modelling

1. Introduction

1.1. Cellular structures and additive manufacturing

Resource efficiency is one of the key considerations in sustainable manufacturing. Additive Manufacturing (AM) is considered a possible option that is able to build parts which optimal designs. Due the manufacturability, complex geometry can be built as the AM builds parts by adding material layer by layer. The design can be optimised in many ways. These days, cellular structures have been brought into attention due to the manufacturing capability of AM. Cellular structures are one of the solutions for reducing material and energy usage. According to the geometry of unit cells and space between them, material usage can be reduced while the parts remain functional.

Cellular structures are complex geometries consisting of a large number of *unit cells* joining with a repetitive pattern. The properties of the structure are determined by the geometry of the unit cell. Cellular structures are generally used as support structures in additive manufacturing. They can also be used to modify certain parts of models to achieve specific properties - namely *stiffness*, *strength*, *compliance*, *thermal*, *dynamic*, and *visual* - which can be determined by the geometry, dimension, and arrangement of the cells [1].

1.2. Problem in modelling and design

According to 3D modelling and representation, two types of techniques, namely *Boundary Representation* (B-Rep) and *Stereo Lithography* (STL), are involved.

B-Rep is a well-established technique for solid geometry modelling that is commonly used in Computer Aided Design (CAD) software. The geometry and topology of the model can be formulated by defining mathematical functions with limits and constraints. For STL, it is known as a standard format for AM. STL represents a model with a surface geometry which is a collection of polygons connected to each other.

The problems in design and modelling arise due to the complexity of the structures regarding the following aspects, *size*, *parameterisation*, *manufacturability*, *precision and validity* [2, 3]. B-Rep can be modified and parameterised easier than STL. However, STL is capable of handling highly

doi:10.1016/j.procir.2016.03.148

complex geometry more efficiently than B-Rep. [4] proposed Hybrid Geometry Modelling (HGM) method that resolves those problems. The unit cell of the model can be parameterised with B-Rep technique before constructing the entire structure and storing as STL. For generating structures with a large number of cells, the performance is improved in Prefabrication Hybrid Geometric Modelling (P-HGM) method [2] (see Section 3.1).

1.3. Cellular structure integration techniques

Much research focuses on the cellular structure generation methods transforming entire base models to cellular structure. [2] used P-HGM to generate uniform large scale uniform structure. [5] used HGM to generate the structure conforming with the base part that is limited to parametric models. [6] used Genetic Algorithm to generate the cellular structure over the entire base part. [7] proposed hierarchy computational models that pack cells along the hosting surface.

Little research has been conducted on the integration process. None of them worked on the automatic approach that integrates the structure to selected areas. Modelling parts with cellular structure integrated in B-Rep and convert to STL is achievable but expensive. Software tools [8-11] that work with polygonal or mesh models directly are more suitable. The structures can be generated automatically but the integration process still needs to be done manually with a number of steps (see Fig. 2(a)).

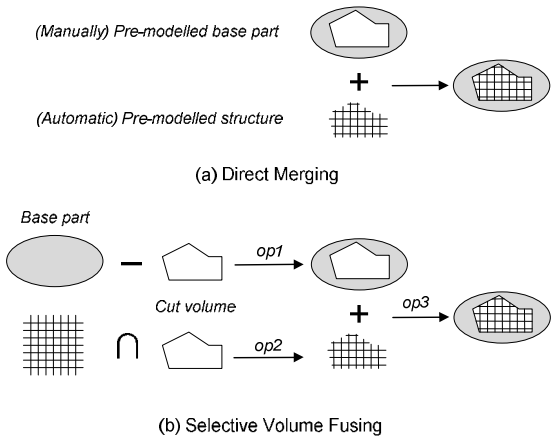

Fig. 1 Surface Boolean operation for part integration

The parts need to be pre-modelled separately and then merged. The volume that will be substituted by cellular structure is manually removed; while the part cellular structure volume can be defined and automatically generated.

1.4. Scope and overview

In this research, the ultimate aim is to develop design software that is able to optimise the design by using cellular structure considering the functional requirement and resource efficiency. The research consists of three development parts; *Phase (1)* - methodology for efficiently generating cellular structure; *Phase (2)* - methodology for automatic integration; *Phase (3)* - methodology for physical properties analysis of the cellular structure integrated parts.

This article focuses the development in Phase (2). An advanced and automatic integration method based on Selective Volume Fusing (SVF) [12], a procedure that facilitates the automatic integration, is presented. A software tool for generating cellular structures and integrating them to the base geometry is developed without considering physical properties of the resultant parts.

This article is organised as follows. The framework of the software tool is presented in Section 2, the methodology in Section 3, implementation and case-study in Section 4, and discussion and conclusion in Section 5.

2. System framework

2.1. Software and libraries

Free Form Design^{TM} (FFD) is a 3D modelling software tool designed for non-experienced CAD users [13]. The cell *cellular structure integration* (CSI) module is developed on FFD platform that is developed in C++ with two libraries. (1) *Visualization Toolkits* (VTK 6.0) [14] is a computer graphic library used for visualisation and modifying surface models, *vtkPolyData*, that can be directly converted to *STL*. (2) *Open Cascade Technology* (OCCT 6.7.1) [15] is a software development kit for solid modelling. The functions are used for geometry modelling in B-Rep. In FFD, B-Rep and STL formats are interchangeable in order to integrate OCCT with VTK (see overview, Fig. 2(e)).

2.2. Cellular structure generation module (CSM)

CSM generate a cellular structure with particular unit cell. The structure is generated rapidly with *P-HGM* [2] (see Section 3.1). The unit cell is modelled in B-Rep with OCCT. The entire structure is created by populating the unit cell by using VTK with polygonal surface model.

2.3. Cellular structure integration (CSI)

CSI integrates the cellular structure generated by CSM with a base part. The proposed method, SVF (see Section 3.2), is used to replace specified volume of the base part with the cellular structure. This process is based on surface Boolean operation of polygon model performed by VTK that can be exported to STL.

3. Methodology

3.1. P-GHM

This section presents a 3D modelling method, P-HGM, hybrid B-Rep – polygonal surface modelling technique that rapidly generates cellular structures. Performance of P-HGM regarding the generation speed is higher in comparison to HGM [4]. The key advantages of HGM are the flexibility in modelling and the minimal computation resources needed in cells joining process that is used for constructing the complete structure. Regarding the joining process, instead of using surface Boolean operation which is a resource intensive

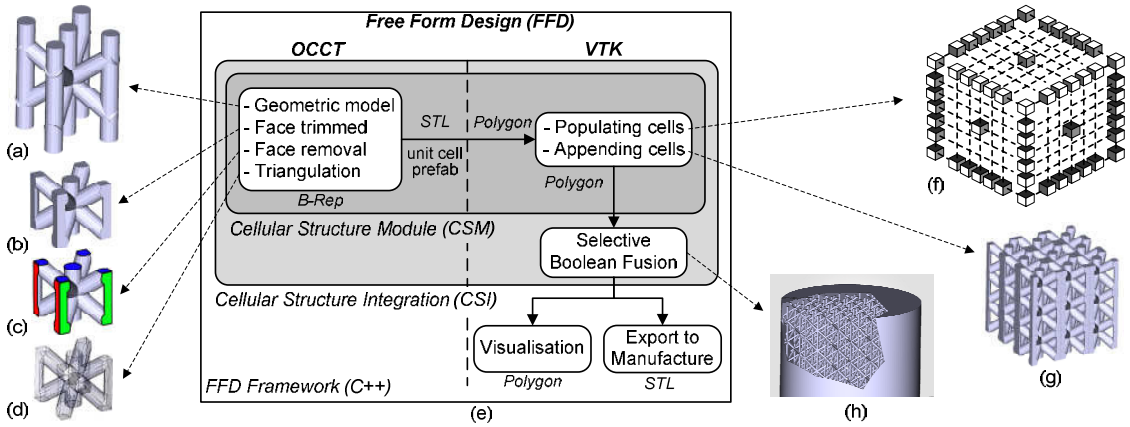

Fig. 2 Framework of CSI and CSM in Free Form Design

process, the cells can be appended directly at the edges of each polygonal face. The edges can be obtained by removing the faces that connect to other cells.

A set of the prefab-cell faces are created based on the cell template with a variation of faces removal pattern, according to the corresponding location of each prefab cell on the final structure [2]. Unlike HGM that generates each cell individually as the populating process goes, P-HGM just places the cells that are already created for particular locations without further calculation. As a result, the process is significantly faster especially for generating large structures where the time is nearly constant regardless of the number of cells generated. P-HGM consists of three primary phases which are summarised as follows (an overview, see Fig. 2).

Phase1: Modelling

A solid model of the unit cell is constructed with a B-Rep technique, which is used as a kernel of most CAD software. In this article, the types of the unit cell are configured based on the cell template in order to ensure the symmetry. Geometry of the model can be easily customised by specifying the control parameters, i.e. cell size, cell type, and beam profile. The template and the unit cell types are illustrated in **Error! Reference source not found.**.

Phase2: Prefabrication of unit cells

A set of prefab-cells will be created in this phase. Considering a final structure which will be enclosed by a rectangular bounding box, the face removal patterns are based on a 3 × 3 cube; therefore, prefab-cells with 27 different patterns need to be generated. Regarding a unit cell in the structure, the connection with other cells will be seamless if the connecting edges are presented while the connecting faces are removed [12].

Constructing each prefab-cell, initially, the unit cell generated from the template (Fig. 2(a)) will be trimmed according to the bounding box represented the distance between cells (Fig. 2(b)). The face remover iterates through the entire cell to locate and remove the faces. This B-Rep unit cell will be triangulated and transform to an STL form (Fig. 2(d)). Eventually, these 27 prefab-cells will be placed at particular locations in the complete structure.

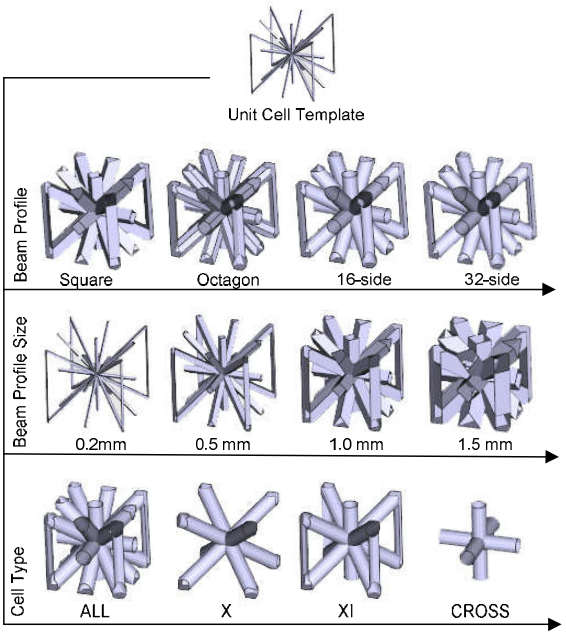

Fig. 3 Variations of unit cell template

Phase3: Creating output structure

The prefab-cells will be populated and appended over the entire volume of the desired complete structure by placing at the corresponding locations (Fig. 2(f)). The structure in an STL format now has been created (Fig. 2(g)).

3.2. Selective volume fusing

SVF is a 3D modelling function that modifies the base part by substituting a specified cutting volume – in this case, a polygonal prism – with a cellular structure created by CSM (see Fig. 2(h)). The substitution is done with a sequence of

surface Boolean operations. In order to reduce complexity in 3D spatial perception for the designers, a 3D polygonal prism is created by extruding a 2D polygon contour in which the user draws it on a virtual plane parallel to the computer screen. The user can specify the contour with offset and the extruding dimension. As a result, the modelling steps can be reduced and simplified according to the main purpose of FFD.

The surface Boolean operation is applied in 3 steps (see Fig. 2(b)). First, (*Op-1*): the specified cutting volume is subtracted from the base part. Concurrently, (*Op-2*): The cellular structure is intersected with the cutting volume. The cavity resulted from *Op-1* will be exactly the same size as the structure produced from *Op-2*. Finally, (*Op-3*): The parts from *Op-1* and *Op-2* will be merged. However, the problem due to co-planar in the surface Boolean operation can be occurred. To avoid this issue, the cellular structure can be enlarged in every direction with minimal value (e.g. 0.001 mm) that will not affect the built quality in the manufacturing process.

Contour offset - The virtual plane-*uv* is determined by the normal vector ($\mathbf{n}^{uv}$) pointing toward the screen. The contour is a spline ($\boldsymbol{S}^{uv}$) constructed from series of the user's specified vertices. The user is able to place the vertices on the surface of the base part ($\mathbf{p}^{xyz}{}_i$) by locating the points on the plane-*uv* ($\mathbf{p}^{uv}{}_i$). The point on plane-*uv* will project to the surface of the base part by ray casting. Another virtual plane-*u´v´* which is parallel to plane-*uv* will be created at the centre of the vertices $\mathbf{p}^{xyz}{}_0$, $\mathbf{p}^{xyz}{}_1$, ... $\mathbf{p}^{xyz}{}_n$ along vector $\mathbf{n}^{uv}$ direction (axis-*w*). This plane is used as a reference plane for profile extrusion.

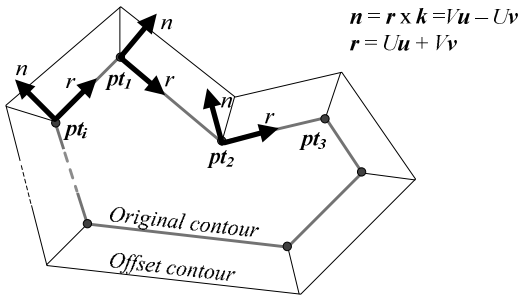

Fig. 4 Vector representation of contour offset

The extrusion is specified by this contour in accordance with three parameters: (a) length in $\boldsymbol{w}^{+}$, (b) length in $\boldsymbol{w}^{-}$, and, (c) contour offset in *uv*-space. The dimension in $\boldsymbol{w}^{+}$ and w^{-} can be specified explicitly. Regarding the contour offset, the offset spline ($\boldsymbol{S}^{uv}{}_D$) will be generated by offsetting each vertex $\mathbf{p}^{uv}{}_i$ in the $\boldsymbol{S}^{uv}$ by the distance D along the vector $\mathbf{n}_{\mathrm{Di}}$ which is a unit vector equally dividing the angle between two connected segments (see Eq(1)). As a result, the new contour will be shifted parallel to each side of the original contour (Fig. 4).

$$\mathbf{p}^{uv}_{Di} = \mathbf{p}^{uv}_{i} + \mathrm{D}\cdot\mathbf{n}_{Di} \tag{1}$$

Where

$$\mathbf{n}_{Di} = \frac{\mathbf{n}_{(i-1)(i)} + \mathbf{n}_{(i)(i+1)}}{\left|\mathbf{n}_{(i-1)(i)} + \mathbf{n}_{(i)(i+1)}\right|}$$

Given that $\mathbf{r}_{fg}$ is a unit vector pointing from point *f* to *g*, the normal vector $\mathbf{n}_{\mathrm{fg}} = \mathbf{r}_{\mathrm{fg}} \times \boldsymbol{w}$ where $\mathbf{r}_{fg} = (\mathrm{U}_g - \mathrm{U}_f)\mathbf{u} - (\mathrm{V}_g - \mathrm{V}_f)\mathbf{v}$. Therefore $\mathbf{n}_{(i-1)(i)}$ and $\mathbf{n}_{(i)(i+1)}$ can be written as Eq(2) and Eq(3).

$$\mathbf{n}_{(i)(i+1)} = \frac{(V_{i+1}-V_i)\mathbf{u} - (U_{i+1}-U_i)\mathbf{v}}{\sqrt{(V_{i+1}-V_i)^2 - (U_{i+1}-U_i)^2}} \tag{2}$$

$$\mathbf{n}_{(i-1)(i)} = \frac{(V_i-V_{i-1})\mathbf{u} - (U_i-U_{i-1})\mathbf{v}}{\sqrt{(V_i-V_{i-1})^2 - (U_i-U_{i-1})^2}} \tag{3}$$

4. Implementation

4.1. Implementation in VTK

The operations presented in Section 3.2 are mesh-based operations performed with VTK library in FFD. The operation workflow consists of 4 steps (see Fig. 5):

Step1: Draw contour on 2D plane

The user can draw a 2D contour by placing the control points on the base part (see Fig. 5(a)). The virtual plane is constructed from a normal vector pointing to the user's screen and ray casting of the starting point on the base part. These points are represented by *vtkPoints* and stored in *vtkPolyData*.

Step2: Generate 3D cutting volume

The contour in Step1 is stored in *vtkPolyData* will be extruded according to the specified length $\boldsymbol{w}^{+}$ and $\boldsymbol{w}^{-}$ and contour offset (see Fig. 5(b)). This cutting volume is generated by *vtkExtrusionFilter* applied to this contour.

Step3: Generate cellular structure with CSM

Cellular structure generated with P-HGM by using OCCT as explained in Section 3.1. CSM is used through a graphical user interface (GUI) that the user can select the type of the unit cell, beam profile and thickness, and size of the unit cell (see Fig. 5(c)). The size of the output structure is determined by the size of the cutting volume according to the bounding box. The output structure is in the form of *vtkPolyData*.

Step4: Merge part and visualisation

Surface Boolean: *vtkBooleanOperationPolyDataFilter* with options *Add*, *Intersection*, and *Subtract* are performed according to steps in shown in Fig. 2(b) to obtain the final part (Fig. 5(d)-(e)). The pipeline in VTK is illustrated in Fig. 6. The merged part is in the form of *vtkPolyData* that possibly contains certain artefacts – i.e. duplicated triangles, inverted normal vectors, bad edges. These can be fixed by applying *vtkCleanPolyData* and *vtkCleanPolyDataFilter*. The merged part has become watertight.

Next, the part will be assigned to the rendering pipeline for visualisation, which is in this order. A *vtkPolyData* contains the data of the merged part. The *vtkPolyDataMapper* maps the data to the graphic primitives. The *vtkActor* displays the object consisting of graphic primitives in the scene. Regarding the size of complex structures consisting of a large number of polygons, levels of detail actor *vtkLODActor* is used instead of *vtkActor* in order to efficiently manipulate and visualise models [14]. The actor will be rendered by *vtkRenderer* which is mapped to display in the *vtkRendererWindow*.

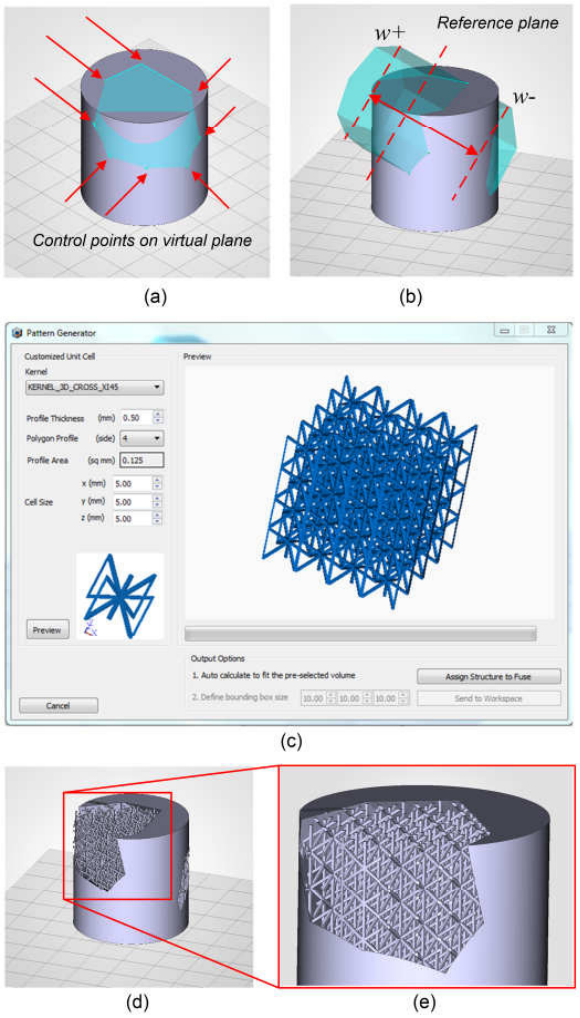

Fig. 5 Workflow of CSM

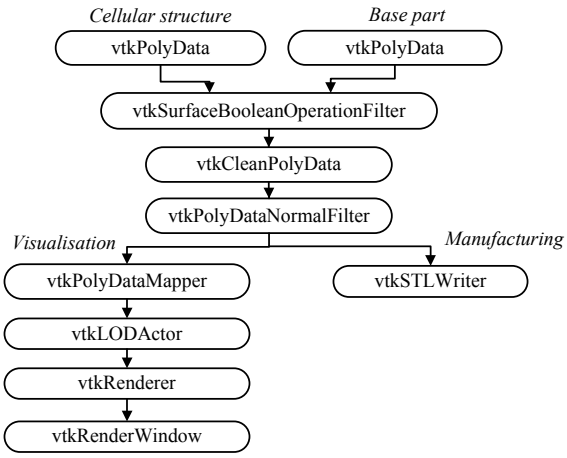

Fig. 6 VTK visualization pipeline

4.2. Case study

The experiments were done in two cases, case-1 (head model) and case-2 (hand model), where the models were selected according to the complexity of geometry (see Fig. 7 and Table 1). The structures were integrated to the base parts by substituting selective volumes, while the selected functional features of the models – the face and the fingers, respectively – remain the same. These cases aim to show the implication of SVF and performance in regard to processing time and resource consumption.

Case-1 was simpler than case-2 due to the size of the volume, the number of cells (504 and 4,200), and the number of triangles (77k and 520k). The purpose of the experiments is to observe two phases of the process, which are cellular structure generation and integration. The performance was indirectly measured from the processing time.

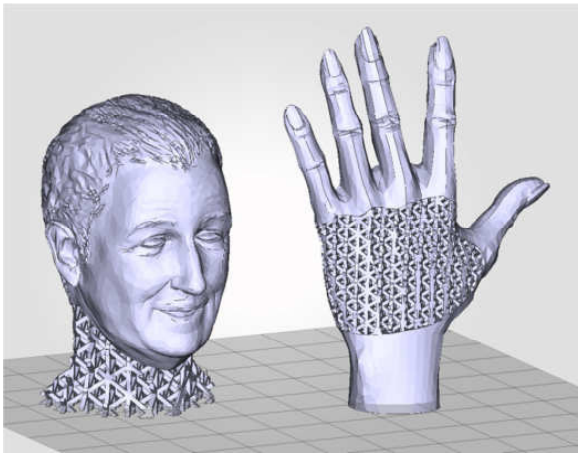

Fig. 7 Case study models: (left) case-1 and (right) case-2

Table 1: Case study properties

	Case-1	Case-2
Base part		
Dimension *(mm)*	40 × 41 ×56	60 ×21×76
Number of triangles	16308	6778
Volume *(mm^3)*	3.422 E+4	1.597 E+4
Building time *(mins)*	301	390
Cellular structure		
Type and beam profile	XI, square	X, square
Number of beam	18	8
Beam thickness *(mm)*	1	1.5
Cell dimension *(mm)*	4 × 4 × 4	4 × 4 × 4
Number of cells	504	4200
Number of triangles	77208	519040
Volume / 1cell *(mm^3)*	13.75	22.5
Volume reduction *(%)*	78.52%	64.84%
Processing time *(s)*	0.27	0.52
Final part		
Number of triangles	48894	103008
Volume *(mm^3)*	2.843 E+4	1.094 E+4
Volume reduction *(%)*	16.91%	31.50 %
Processing time *(s)*	20.47	52.33
Building time *(mins)*	303	394

First, for the structure generation using P-GHM, the processing time was less than 0.6s which was an insignificant difference in both cases, in comparison to the considerably different number of cells generated [10].

Second, the performance of the SVF is related to the complexity of the joining area between both parts. The complexity can be indirectly determined with the number of triangles. As expected, the processing time for case-1 was shorter than case-2, 20.47s and 52.33s, respectively.

The results also showed the volume reduction. For the cellular structure, the reduction ratio can be estimated from the properties of the unit cell. In this case, they were calculated directly from the model, e.g. around 80% and 65% for case-1 and case-2. For final parts, the reduction ratio also depended on the size of selected volume. As a result, the ratios were approximately 17% and 32%, respectively, which refer to the percentage of material saving.

4.3. Manufacturing

The sample parts were manufactured with Selective Laser Sintering (SLS) method. The experiments were done on EOS380 Machine with material Polyamide (PA2200) powder. SLS was selected for manufacturing cellular structure integrated objects in this experiment due to the finest building resolution (10 microns) and does not need support structures. The time for building the base parts were compared to the time for building the cellular structure integrated samples. From Table 1, the building time between two cases was insignificant, 301-303 mins for case-1 and 390-394 mins for case-2.

These preliminary experiments show that the time did not decrease as expected. In SLS process, the time for operating mechanical parts, e.g. movement of powder roller, dominates the material related process, e.g. curing time at each point of the object. The laser strip as a scanning line passes through the projection of the object at each layer. Hence, the processing time will be the same for the objects having similar size of bounding box at each layer, regardless of the shape. The, the time consumption may reduce in other AM techniques where the material processing time is significant. For example, in Fused Deposition Modelling (FDM), the extruder needs to go through every single point of the object and melt the material. The reduction of time and energy are expected to occur.

5. Conclusions

This research works on the development of a software tool for utilisation of cellular structures generated with P-HGM. This article focuses on SVF-based integration method that is capable of substituting the cellular structure part into an arbitrary user-defined geometry on the base part. This method allows the user to design cellular structure integrated objects more intuitively, where more complicated steps are needed in commercial design software tools. These methods are implemented with VTK and OCCT under FFD platform.

From the case study, these methods are capable of producing parts as desired. The material usage decreased according to the qualification of the cellular structure as expected. However, the time consumption was not reduced in SLS process since the movement of printing mechanism dominate the material processing time, hence the energy consumption. While the material usage can be obviously reduced, reduction of energy consumption still cannot be seen when using SLS. The energy and time consumption are expected to exhibit the material processing time is significant.

The modelling method has been achieved without concerning the functionality yet. For the future work, mechanical properties especially strength of the parts will be taken into account. Finite Element Analysis (FEA) will be performed on types of cellular structures and cellular structure integrated objects. In-depth analysis on the manufacturing point of view will be performed. Eventually, modelling software with an expert system that helps users selecting types and geometry of unit cells for required specific purposes will be developed.

Acknowledgement

This research is part of a project Free Form Design which is mainly funded by Advanced Manufacturing Service, Breseight Pty, Ltd, Australia. The research regarding the design and manufacturing cellular is partially supported by Tech Voucher program, New South Wales Government, Australia, under grant number 01182228.

References

[1] Doubrovski Z, Verlinden JC, Geraedts JMP, editors. Optimal design for additive manufacturing: opportunities and challenges. ASME Design Engineering Technical Conference; 2011.
[2] Vongbunyong S, Kara S. Rapid generation of uniform cellular structure by using prefabricated unit cells Int J Comput Integr Manuf. 2015;(In Review).
[3] Pasko A, Vilbrandt T, Fryazinov O, Adzhiev V, editors. Procedural function-based spatial microstructures. SMI 2010 - International Conference on Shape Modeling and Applications, Proceedings; 2010.
[4] Wang H, Chen Y, Rosen DW, editors. A hybrid geometric modeling method for large scale conformal cellular structures. Proceedings of the ASME International Design Engineering Technical Conferences and Computers and Information in Engineering Conference - DETC2005; 2005.
[5] Graf GC, Chu J, Engelbrecht S, Rosen DW, editors. Synthesis methods for lightweight lattice structures. Proceedings of the ASME Design Engineering Technical Conference; 2009.
[6] Mahdavi SH, Hanna S, editors. Blurring the boundaries between actuator and structure: Investigating the use of stereolithography to build adaptive robots. 2004 8th International Conference on Control, Automation, Robotics and Vision (ICARCV); 2004.
[7] Duro-Royo J, Zolotovsky K, Mogas-Soldevila L, Varshney S, Oxman N, Boyce MC, et al. MetaMesh: A hierarchical computational model for design and fabrication of biomimetic armored surfaces. Computer Aided Design. 2015;60:14-27.
[8] Materialise. Magics, the Most Powerful 3D Printing Software [cited 2015]. Available from: http://software.materialise.com/magics.
[9] Autodesk. AutoDesk Within Medical 2015 [cited 2105]. Available from: http://www.withinlab.com/software/new_medical.php.
[10] Netfabb. [cited 2105]. Available from: www.netfabb.com.
[11] Cignoni P, Granzuglia. MeshLab - A processing system for 3D triangular meshes 2015 [cited 2015]. Available from: http://sourceforge.net/projects/meshlab.
[12] Vongbunyong S, Kara S. Selective volume fusing method for cellular structure integration. Sustainability Through Innovation in Product Life Cycle Design, Proceedings of EcoDesign 2015 International Symposium. 2015
[13] Breseight.Pty.Ltd. Free Form Design™ - Endless Creativity with Effortless Modelling 2014. Available from: http://www.free-form-design.com.
[14] Kitware. VTK - Visualization Toolkits [cited 2013]. Available from: http://www.vtk.org.
[15] Open Cascade S.A.S. Open Cascade Technology [cited 2014]. Available from: http://www.opencascade.org